Membrane Assembly of the 16-kDa Proteolipid Channel from *Nephrops norvegicus* Studied by Relaxation Enhancements in Spin-Label ESR†

Tibor Páli,‡,§ Malcolm E. Finbow,|| and Derek Marsh*,‡

Max-Planck-Institut für biophysikalische Chemie, Abteilung Spektroskopie, Am Fassberg, D-37077 Göttingen, Germany, and Beatson Institute for Cancer Research, Garscube Estate, Bearsden, Glasgow, G61 1BD, U.K.

Received June 25, 1999; Revised Manuscript Received August 13, 1999

ABSTRACT: The 16-kDa proteolipid from the hepatopancreas of *Nephrops norvegicus* belongs to the class of channel proteins that includes the proton-translocation subunit of the vacuolar ATPases. The membranous 16-kDa protein from *Nephrops* was covalently spin-labeled on the unique cysteine Cys54, with a nitroxyl maleimide, or on the functionally essential glutamate Glu140, with a nitroxyl analogue of dicyclohexylcarbodiimide (DCCD). The intensities of the saturation transfer ESR spectra are a sensitive indicator of spin−spin interactions that were used to probe the intramembranous structure and assembly of the spin-labeled 16-kDa protein. Spin−lattice relaxation enhancements by aqueous Ni^{2+} ions revealed that the spin label on Glu140 is located deeper within the membrane (around C9−C10 of the lipid chains) than is that on Cys54 (located around C5−C6). In double labeling experiments, alleviation of saturation by spin−spin interactions with spin-labeled lipids indicates that spin labels both on Cys54 and on Glu140 are at least partially exposed to the lipid chains. The decrease in saturation transfer ESR intensity observed with increasing spin-labeling level is evidence of oligomeric assembly of the 16-kDa monomers and is consistent with a protein hexamer. These results determine the locations and orientations of transmembrane segments 2 and 4 of the 16-kDa putative 4-helix bundle and put constraints on molecular models for the hexameric assembly in the membrane. In particular, the crucial DCCD-binding site that is essential for proton translocation appears to contact lipid.

The 16-kDa proteolipid that is isolated from the hepatopancreas of the lobster *Nephrops norvegicus* bears a strong sequence similarity with the proteolipid subunit *c* of the vacuolar H^+-ATPases (V-ATPase)[1] (*1*). Expression in yeast shows that the *Nephrops* 16-kDa proteolipid is able to substitute functionally for the vacuolar proteolipid in a hybrid V-ATPase that is sensitive to DCCD (*1*, *2*). The endogenous 16-kDa proteolipid, encoded by the *VMA3* gene in yeast, is the major component of the transmembrane V_o-sector of the V-ATPase, which contains a minimum of four copies of the *vma3p* proteolipid and one copy each of homologous proteolipids encoded by the *VMA11* and *VMA16* genes (*3*, *4*). The *vma11p* and *vma16p* proteolipids (subunit c′ and c″) have 80 and 20% homology, respectively, with the major 16-kDa proteolipid. The DCCD-reactive site that is essential for proton translocation is a carboxyl-containing residue that is conserved throughout the proteolipid subunits of the vacuolar and mitochondrial proton ATPases.

The 16-kDa proteolipid from *Nephrops* can be isolated as two-dimensional arrays of paired membranes, which bear a resemblance to gap junctions. Other components of the V_o-sector, including the single-copy proteolipids, are absent. On the basis of electron microscopy, atomic force microscopy, and sequence analysis, the channel structures formed by the proteolipid have been modeled as hexameric assemblies of 4-helix transmembrane bundles (*3*, *5*). Support for this overall structure has been obtained from low-resolution electron crystallographic projections, together with Fourier transform infrared spectroscopy (*1*). The stoichiometry and specificity of the lipid−protein interactions of the *Nephrops* proteolipid determined by spin-label ESR spectroscopy are also consistent with the proposed model for the oligomeric assembly (*6*). Mutational analysis and cysteine-labeling studies on the hybrid V-ATPase have demonstrated that the features proposed for the orientation of the channel-lining helix 1 in the molecular model are present in the intact vacuolar system (*7*). Also, the binding of a fluorescent dibutyltin-flavone complex to the 16-kDa protein in a heterologously expressed hybrid vacuolar ATPase was found recently both

‡ Max-Planck-Institut für biophysikalische Chemie.

|| Beatson Institute for Cancer Research.

† This work was supported in part by a grant from the Volkswagen Stiftung. Travel fellowships from EMBO and FEBS and partial support from the Hungarian National Science Foundation (OTKA T029458) are gratefully acknowledged.

* Corresponding author. Dr. Derek Marsh, Max-Planck-Institut für biophysikalische Chemie, Abt. Spektroskopie, D-37070 Göttingen, Germany. Telephone: +49-551-201 1285. Fax: +49-551-201 1501. E-mail: dmarsh@gwdg.de.

§ Permanent address: Institute of Biophysics, Biological Research Centre, H-6701 Szeged, Hungary.

[1] Abbreviations: V-ATPase, vacuolar H^+-ATPase; DCCD, *N*,*N*′-dicyclohexylcarbodiimide; NCCD, *N*-(2,2,6,6-tetramethylpiperidine-1-oxy)-*N*′-cyclohexylcarbodiimide, 5-MSL, 3-maleimido-2,2,5,5-tetramethylpyrrolidine-*N*-oxyl; n-SASL, *n*-(4,4-dimethyloxazolidine-*N*-oxyl)-stearic acid; TS, 4-octadecanoyl-2,2,6,6-tetramethylpiperidine-1-oxyl; ESR, electron spin resonance; HEPES, 4-(2-hydroxyethyl)-1-piperazineethanesulfonic acid; EDTA, ethylenediamine tetraacetic acid; ST-ESR, saturation transfer ESR.; V_1, first-harmonic absorption ESR spectrum detected in phase with respect to the static magnetic field modulation; V_2', second-harmonic absorption ESR spectrum detected 90°-out-of-phase with respect to the static magnetic field modulation.

10.1021/bi991459c CCC: $18.00
Published on Web 10/07/1999

to inhibit ATPase activity and, most significantly, to be reversed at least partially by DCCD binding (*8*).

In the present work, we have concentrated on fine structural features in the membrane assembly of the *Nephrops* proteolipid. This is done by determining various spin−spin interactions with the spin-labeled protein, by using saturation-transfer ESR spectroscopy. The specific sites of spin-labeling are the unique Cys54 in transmembrane segment 2 that is labeled by maleimide and the essential Glu140 in transmembrane segment 4 that is labeled by DCCD. The intensities of the spin-label ST-ESR spectra are sensitive indicators of the enhancement in effective spin−lattice relaxation rate that arise from spin−spin interactions with paramagnetic ions or with other spin labels (*9*). Here, aqueous Ni^{2+} ions are used to determine the distance of the spin-labeled residues from the membrane surface (*10*, *11*). Spin-labeled lipids are used to assess the exposure of the spin-labeled residues to the hydrophobic lipid phase (*12*). Spin−spin interactions between adjacent spin-labeled monomers are used to detect oligomerization. These measurements determine the location and orientation of the transmembrane segments to which the spin labels are attached. Of especial significance is the segment bearing the DCCD-reactive residue that is involved in proton transport.

MATERIALS AND METHODS

Isolation of 16-kDa Membranes. Membranes containing the 16-kDa channel proteolipid were isolated from the hepatopancreas of the decapod *Nephrops norvegicus* either by detergent extraction (Triton X-100 and *N*-lauroyl sarcosine) or by extraction with NaOH (25 mM) as previously described (*3*, *6*, *13*, *14*). After extraction, the enriched membranes were digested with trypsin and suspended in 6 M urea before separation on sucrose step gradients.

N-Ethylmaleimide Labeling of 16-kDa Protein. Membranes (approximately 0.25 mg protein) were suspended in 50 μL of H_2O containing 0.037 MBq of [^{14}C]-*N*-ethylmaleimide (Amersham plc, U.K.). The membranes were left for 16 h at room temperature in the dark before pelleting in a microfuge and suspending in SDS buffer for SDS-PAGE. SDS gels were stained in Coomassie brilliant blue and autoradiographs were prepared from dried gels. The gels and autoradiographs were scanned (Molecular Dynamics Laser Scanner) to quantitate the ratio of monomeric and dimeric forms of the 16-kDa proteolipid and labeling of the two forms.

Spin Labeling. Spin-labeled maleimide (5-MSL) was obtained from Syva (Palo Alto, CA), and the spin-labeled DCCD derivative (NCCD) was prepared according to refs *15* and *16*. All buffers and sample capillaries used in nonlinear ESR experiments were carefully deoxygenated and saturated with argon. Sarcosyl-extracted membranes from *Nephrops* were washed with 10 mM HEPES, 10 mM NaCl (pH 7.8), after extensive pre-washing with 10 mM HEPES/EDTA, if required, to remove endogenous copper. Spin label solutions were corrected for the differences in their specific activities, as assayed by EPR.

For experiments with different fractions of spin-labeled monomer, the 16-kDa protein was labeled by adding different volumes of (excess) 5-MSL dissolved in EtOH (10 mg/mL), and then incubating the membrane dispersion (1−5 mg/mL) for ca. 1 h at room temperature. Unbound label was removed by repeated washing with fresh buffer. The fraction of the nonspecific labeling increased with increasing amounts of spin label added.

For experiments involving paramagnetic ion-induced quenching, a similar method of labeling was used for 5-MSL and NCCD, except that incubation with NCCD was at 45 °C and only samples with low label/monomer ratios were used. After removal of unbound label, membranes were repeatedly washed in buffer containing the required amount of $NiCl_2$ or Ni-EDTA, by centrifuging three times in the ESR capillary, without removing the membrane pellet between washes. Alternatively, membranes were labeled with TS or n-SASL by using a similar procedure, except that the samples were incubated at 45 °C for 1 h, followed by overnight incubation at room temperature. In addition, only one washing step was used after labeling with TS or n-SASL.

For doubly labeled samples, the prewashed material was divided into two parts. One part was labeled with 5-MSL or NCCD as described above. The other part was further divided for control labeling with the lipid labels TS or n-SASL, separately. The ESR spectra of the singly labeled samples were recorded in order to determine the exact label content of each aliquot. The protein-labeled sample was then washed back into the original tube and further divided into aliquots, for labeling separately with the different lipid labels. This final step for the double-labeled samples was performed as for the control samples that were singly labeled with TS or n-SASL. The final labeling level with n-SASL was in the region of 1.5−3.5 mol %, relative to total membrane phospholipid plus cholesterol. This level of labeling was required approximately to maximize mutual spin−spin interactions between labeled lipid and labeled protein.

ESR Spectroscopy. Typically 0.5−1 mg of membrane material was concentrated for measurement in 1 mm i.d. ESR capillaries. Excess supernatant was removed to obtain a sample length of 5 mm according to the standard protocol for ST-ESR measurements (*17*). Phospholipid and protein content in the ESR samples was determined by phosphate (*18*) and protein assays (*19*). EPR measurements were performed on a Varian Century Line 9-GHz spectrometer equipped with gas-flow-temperature regulation and interfaced to a personal computer. Nominal microwave power was calibrated against microwave H_1-field at the sample and cavity Q, as described earlier (*20*). All measurements were carried out under critical coupling conditions with a scan range of 100 G, unless indicated otherwise. After phase setting by the self-null method, saturation transfer ESR spectra (V_2'-display) were recorded with a 50 kHz field modulation, a modulation amplitude of 5.0 G and 100 kHz phase-quadrature detection (*17*). Both V_1- and V_2'-spectra were corrected either with a linear baseline or with a blank spectrum from a nonlabeled sample. The first integral of the V_2'-signal was normalized by the second integral of the V_1-signal (conventional first-derivative ESR spectrum) recorded at the same microwave power, but with a field modulation of 1.25 G, to give the normalized saturation transfer intensity, I_{ST}.

Absolute spin concentration was determined by comparing the normalized second integral of the low-power ($H_1 = 0.083$ G) V_1-spectra with a DPPH standard, which in turn was standardized spectrophotometrically, as described elsewhere

(*21*). Line widths of the low- and high-field extrema of the conventional V_1-spectra were determined by local fitting with Lorentzian line shapes. Low-power V_1-spectra recorded from double-labeled samples at 45 °C were fitted to a superposition of spectra from corresponding singly labelled samples, to obtain the relative double-integrated intensities of the constituent components.

RESULTS AND DISCUSSION

Characterization of Labeling Specificity of the 16 kDa Proteolipid. The *Nephrops norvegicus* 16-kDa proteolipid contains a single cysteine residue (Cys54) and a previous study (*7*) has shown that this residue is reactive to maleimide reagents. The proteolipid migrates on SDS-PAGE gels as monomeric and dimeric species (*13*), and quantitative scanning of Coomassie-stained gels shows that the dimer/monomer ratio is 0.68 ± 0.05 ($n = 3$). The dimer is not dissociated by the addition of reducing agents. Autoradiography of gels from membranes incubated with [^{14}C]-*N*-ethylmaleimide (NEM) shows that the proteolipid is the only reactive protein. However, the dimeric species is poorly labeled by NEM, and quantitative scanning shows that the dimer/monomer labeling ratio is 0.19 ± 0.08 ($n = 3$). This suggests that, in the isolated membrane arrays, there are two forms of the proteolipid in the hexameric complexes, of which the minor form (seen as the dimeric species on SDS-PAGE) is not fully accessible to reaction with NEM. Taking this into consideration, the maximal labeling by NEM of the 16-kDa proteolipid would be close to a fraction of 0.7. Previous studies with radio-labeled DCCD have demonstrated that Glu140 of the 16-kDa proteolipid is the sole reaction site for DCCD with the *Nephrops* membrane preparations (*3*).

ESR and ST-ESR Spectra of Spin-Labeled 16-kDa Proteolipid. The conventional V_1 ESR spectra of the maleimide-(5-MSL) labeled 16-kDa proteolipid membranes are given as a function of the spin label/protein monomer mole ratio in Figure 1. The different levels of spin labeling were achieved by varying the concentration of 5-MSL label in the reaction mixture and the degree of spin-labeling was determined by double-integrating the ESR spectra, together with chemical analysis of the membrane protein content (see Materials and Methods). For the latter, it was assumed that all of the residual membrane protein was the 16-kDa proteolipid (see above), and the sequence molecular weight was taken as 17 000 kDa (*3*).

It is seen from Figure 1 that there is little difference between the conventional ESR spectra at different levels of spin-labeling, apart from trivial effects of signal/noise ratio and the presence of a small, sharp three-line signal that appears at higher labeling levels. This latter spectral component is attributed to nonspecific labeling, but the total integrated intensity associated with it remains low, relative to the total integrated intensity, even at the highest levels of spin-labeling achieved. The spectra were recorded at a relatively low temperature and the major signal, which is attributed to specific labeling by the maleimide spin label derivative at the single unique cysteine (Cys54) residue in the native protein, corresponds to a single-component powder pattern. This spectral component has a large outer hyperfine splitting of 67.5 G, which is close to the rigid limit value,

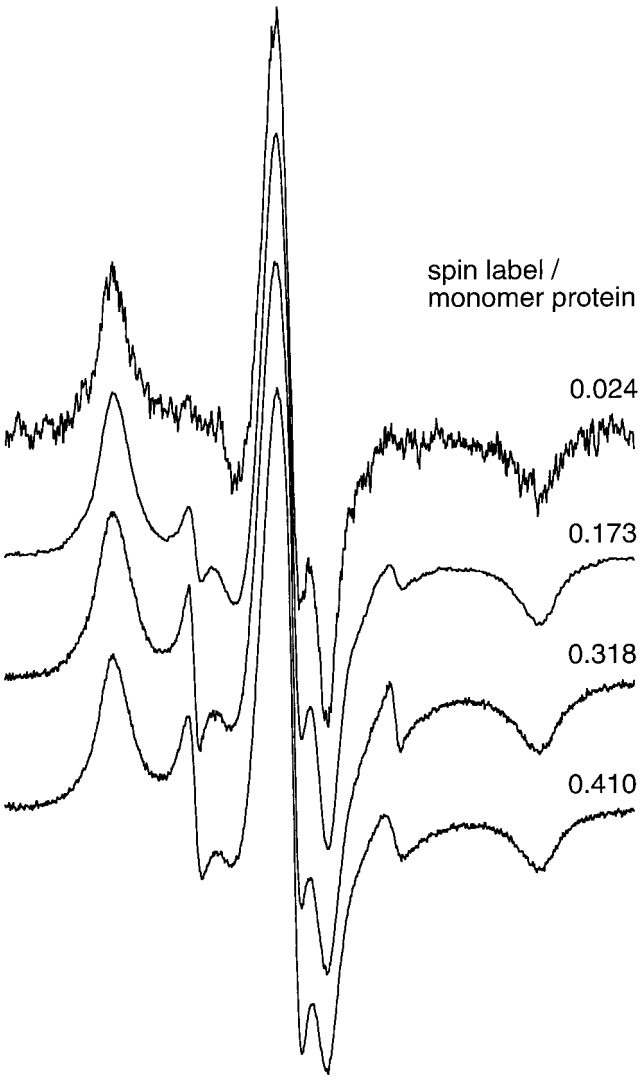

FIGURE 1: Conventional first-harmonic, in-phase absorption ESR spectra (V_1-display) of membranous 16-kDa proteolipid from *Nephrops norvegicus* covalently spin-labeled with the maleimide derivative, 5-MSL. From top to bottom: spectra are shown with increasing levels of spin-labeling at 5-MSL/protein mole ratios indicated in the figure. $T = 5$ °C, total scan width = 100 G.

and, therefore, evidences little or no rapid independent segmental motion of the protein-bound spin label, at this particular temperature. The effective segmental correlation times obtained from the outer line widths are $\tau_R^{seg} \geq 40-70$ ns, assuming a rigid limit peak-to-peak line width of $\delta = 3.0$ G (*22*). Overlaying the various spectra corresponding to increasing levels of spin-labeling indicates that there is no detectable increase in line width arising from spin−spin interactions, within the range of sensitivity of the conventional ESR spectra. Observation of any weak spin−spin interactions between spin-labeled monomers, on increasing the level of monomer labeling, therefore, requires a more sensitive means to detect spin−spin interactions. This is afforded by the saturation properties of the spin label spectra − in this case by the nonlinear saturation transfer ESR spectra (see ref *23*).

The second-harmonic, out-of-phase V_2' ST-ESR spectra that correspond to the different levels of spin-labeling, for which the conventional V_1 ESR spectra were given in Figure 1, are presented in Figure 2. In this case, apart from the presence of sharp nonspecific spectral components that again

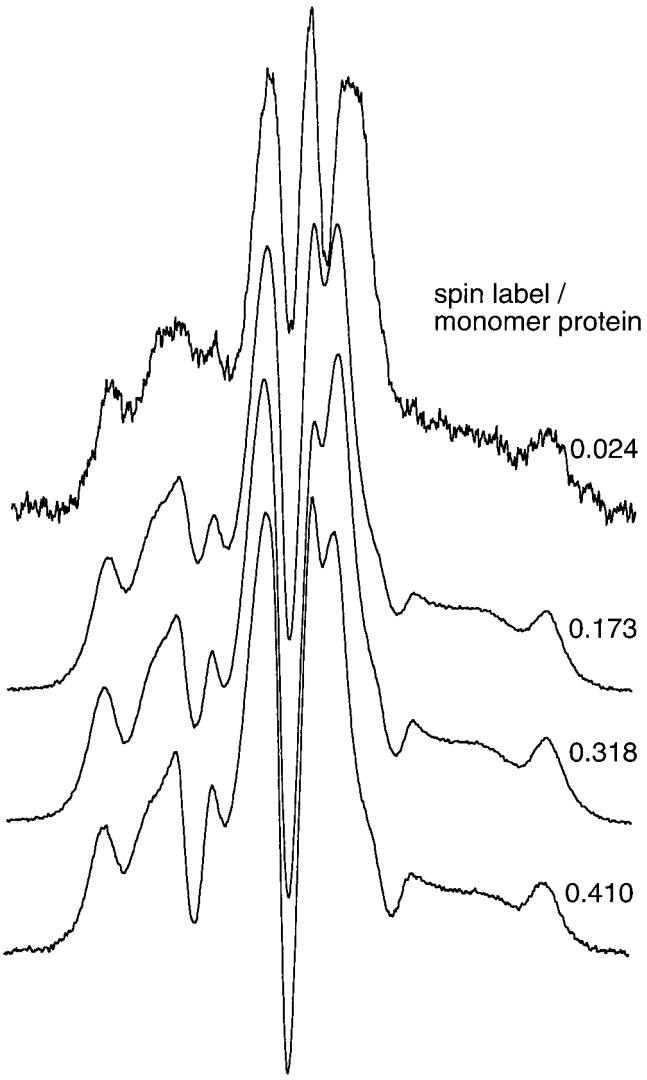

FIGURE 2: Second-harmonic out-of-phase, absorption saturation-transfer ESR spectra (V_2'-display) of membranous 16-kDa proteolipid from *Nephrops norvegicus* covalently spin-labeled with the maleimide derivative, 5-MSL. From top to bottom: spectra are shown with increasing levels of spin-labeling at 5-MSL/protein mole ratios indicated in the figure. $T = 5$ °C, total scan width = 100 G.

appear at the higher levels of spin-labeling and obscure the central regions of the main spectral component, the ST-ESR spectra do exhibit some slight changes in line shape in the outer wings of the ST-ESR spectra. The major changes that take place in the ST-ESR spectra with increasing labeling level are, however, in the normalized intensities, as will be seen immediately below (cf. ref *23*). The effective rotational correlation times of the spin-labeled 16-kDa proteolipid, that are determined from calibrations of the diagnostic lineheight ratios in the low-field and high-field regions (see refs *24* and *25*) of the ST-ESR spectra are in the region of $\tau_R^{eff} \approx 150-200$ μs. These very long values confirm that there is no large-amplitude segmental motion of the spin label relative to the protein. Very long correlation times are expected because it is known that, in the membranous preparations from *Nephrops* that are produced by extraction with *N*-lauroyl sarcosine, a relatively high proportion of the protein is present in two-dimensional arrays (*1*, *3*).

Dependence on Spin-Labeling Level. The reduction in intensity of the ST-ESR spectrum with increasing fraction, *F*, of 16-kDa monomers that are spin-labeled arises from

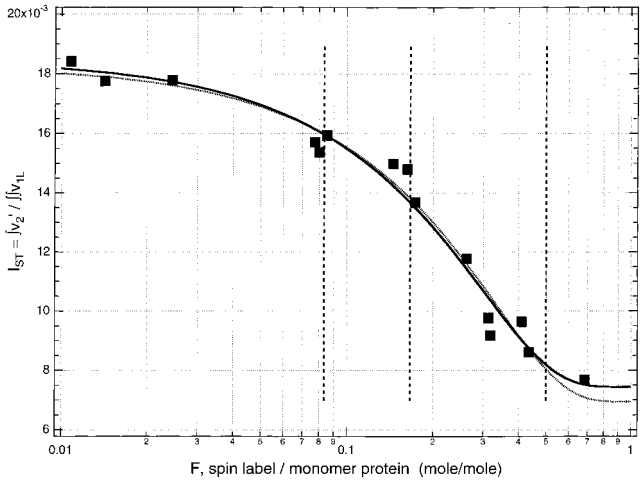

FIGURE 3: Dependence of the integrated intensity, I_{ST}, of the V_2' ST-ESR spectra of membranous 16-kDa protein spin-labeled with 5-MSL on the level of labeling. The ST-ESR intensity is normalized effectively to the number of spins by using the second integral of the conventional V_1-ESR spectrum recorded at subsaturating power, which is also used to determine the average fraction, *F*, of spin labels per 16-kDa monomer. The dotted line is a nonlinear least-squares fit from eqs 1 and 2 with $N = 6$. Nonlinear optimization with the degree of oligomerization also as a free parameter (solid line) yields a fitted value of $N = 6.6 \pm 0.7$.

intermolecular spin−spin interactions between spin-labeled monomers in the channel assemblies. The dependence of the ST-ESR intensity on the level of spin-labeling can be modeled by assuming that oligomers containing more than one spin-labeled monomer contribute an intensity, I_{ST}', that is reduced relative to the value I_{ST}^o for the isolated spin-labeled monomer. The net normalized ST-ESR intensity observed is then given by:

$$I_{ST} = (I_{ST}^o - I_{ST}')\frac{p_1}{1 - p_0} + I_{ST}' \qquad (1)$$

where p_n is the probability that *n* monomers are labeled in the oligomeric assembly. The term $(1 - p_0)$ in the denominator of eq 1 arises because the intensity is normalized to the total number of spin labels. For a statistical distribution of labels among the *N*-mers, the labeling probabilities are given by the binomial distribution:

$$p_n = \frac{N!}{n!(N-n)!}F^n(1-F)^{N-n} \qquad (2)$$

where *N* is the number of monomers in the assembly and $\sum_{n=0}^{N} p_n = 1$.

From Figure 3, it is seen that the dependence of the normalized ST-ESR intensity on the extent of spin labeling can be described fairly well by means of eqs 1 and 2 with $N = 6$. The maximum level of spin-labeling that was achieved experimentally corresponded to $F \sim 0.7$ per monomer, in agreement with the calculated maximum labeling by NEM. This is sufficient to determine the size, *N*, of the assemblies from the ST-ESR data with a reasonable degree of accuracy. Releasing the degree of oligomerization as a nonlinear fitting parameter yields a value of $N = 6.6 \pm 0.7$, which is consistent with a hexameric assembly of the 16-kDa monomers.

It will be noted that a binomial distribution of spin-labeled monomers has been demonstrated recently for membrane-assembled annexin XII that consisted of random mixtures of labeled and unlabeled species (*26*). In this latter case, spin−spin interactions were strongly evident even in the conventional ESR spectra and were shown to result from formation of membrane-bound annexin trimers, similar to those found in the crystal structure.

Spin−Lattice Relaxation by Paramagnetic Ions. The normalized intensities, I_{ST}, of the ST-ESR spectra from the spin-labeled protein and spin-labeled fatty acids in 16-kDa membranes were measured with increasing concentrations of aqueous Ni^{2+} ions, or their complex with EDTA, in the water phase. The intensities of the spin-label ST-ESR spectra decrease with increasing Ni^{2+} concentration. This is partly a result of direct Heisenberg-exchange interactions with paramagnetic ion complexes that have a decreasing profile of solubility into the membrane (*10*), and because of distance-dependent magnetic dipole interactions with the fast-relaxing Ni^{2+} ions (*11*). The experiments with fatty acid probes spin-labeled at different positions in the hydrocarbon chain serve as a calibration of the distance from the surface into the membrane. This calibration is used to locate the position of the 5-MSL spin label on residue Cys54 and the NCCD spin label on Glu140, respectively, when these spin labels are bound specifically to the 16-kDa protein.

The enhancements in spin−lattice relaxation with increasing Ni^{2+} concentration are given in Figure 4 for various spin labels in 16-kDa membranes. For the analysis, it is assumed that the ST-ESR integral intensity, I_{ST}, is directly proportional to the spin−lattice relaxation time, T_1. This approximation is found to be the case, both experimentally (*11*, *23*) and theoretically (*9*), over the range of T_1-values that are typical for paramagnetic relaxation enhancements of nitroxide spin labels. Under these conditions, the increase in spin−lattice relaxation rate of the spin label is directly proportional to the paramagnetic ion concentration. The following dependence of the ST-ESR intensity, I_{ST}, on Ni^{2+} ion relaxant concentration, c_R, is, therefore, expected (see ref *27*):

$$1/I_{ST} = 1/I_{ST}^{o} + k_{RL}c_R \qquad (3)$$

where I_{ST}^{o} is the value of I_{ST} in the absence of Ni^{2+} ions, and k_{RL} is a measure of the accessibility or distance of closest approach of the Ni^{2+} ions to the spin label. From Figure 4, it is seen that a linear dependence of $1/I_{ST}$ on c_R, as is predicted by eq 3, is obtained for the Ni−EDTA complex that cannot bind strongly to components of the membrane. In contrast, a biphasic dependence of $1/I_{ST}$ on c_R is obtained for uncomplexed aqueous Ni^{2+} ions. The initial steep dependence of $1/I_{ST}$ on Ni^{2+} concentration (for $[Ni^{2+}] < 4$ mM), in the latter case, corresponds to the specific binding of Ni^{2+} to a divalent metal ion site on the 16-kDa protein. Independent experimental evidence has been obtained for such an endogeneous binding site from the conventional Cu^{2+} ESR spectra of native membranes that have not been washed with EDTA (Páli et al., unpublished).

The gradients of $1/I_{ST}$ with respect to Ni^{2+} ion concentration for the n-SASL spin probes in 16-kDa membranes are plotted in Figure 5 as a function of the position, *n*, of the spin label in the lipid chain. These values of $d(1/I_{ST})/d[Ni^{2+}]$ were determined from data such as those in Figure 4, for

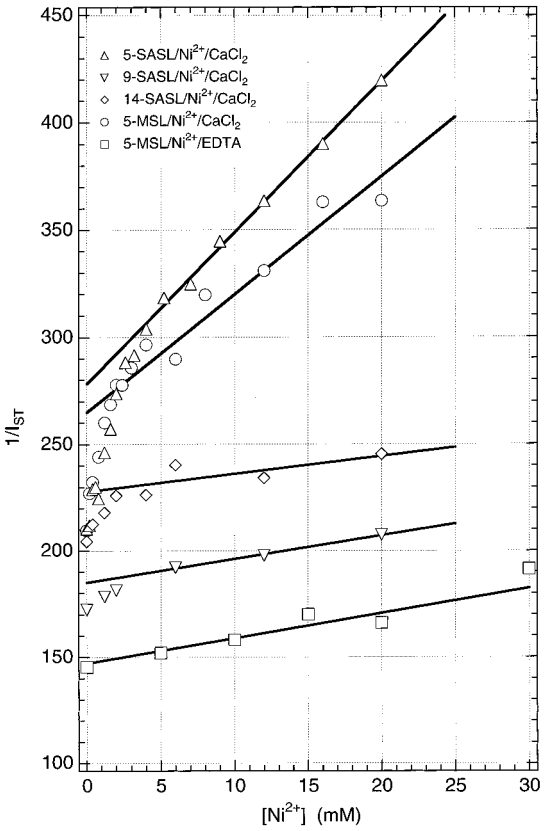

FIGURE 4: Dependence of the reciprocal normalized ST-ESR integral intensity, $1/I_{ST}$, on aqueous Ni^{2+} ion concentration for 16-kDa proteolipid membranes either specifically labeled with 5-MSL (circles or squares), or spin-labeled in the lipid regions of the membranes with various n-SASL stearic acid spin probes (upward and downward triangles). The straight lines are linear regressions for $[Ni^{2+}] \geq 4$ mM. The data for 5-MSL that are given by squares correspond to the Ni-EDTA complex, all other data correspond to free aqueous Ni^{2+}.

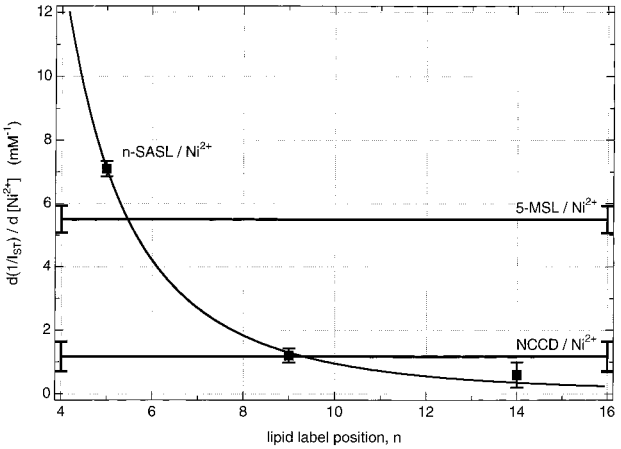

FIGURE 5: Gradient of the dependence of $1/I_{ST}$ on Ni^{2+} ion concentration, $d(1/I_{ST})/d[Ni^{2+}]$ (squares), as a function of label position, *n*, for the different positional isomers, n-SASL, of spin-labeled stearic acid in 16-kDa proteolipid membranes from *Nephrops*. Superimposed as horizontal lines are the values of $d(1/I_{ST})/d[Ni^{2+}]$ for MSL- and NCCD-labeled 16-kDa proteolipid membranes.

Ni^{2+} ion concentrations in the range $[Ni^{2+}] \geq 4$ mM where the specific ion binding is saturated. They correspond to values of k_{RL} in eq 3 for which spin−spin interactions are dependent on the position of the spin label relative to the membrane surface (*10*, *11*). The steadily decreasing effects of the Ni^{2+}-induced paramagnetic relaxation with depth of

the spin label in the membrane, thus provide a calibration of the intramembranous location of the spin-labeled residues on the 16-kDa proteolipid protein. The values of $d(1/I_{ST})/d[Ni^{2+}]$ for the 5-MSL and NCCD spin labels covalently bound to the 16-kDa proteolipid in *Nephrops* membranes are also indicated in Figure 5. It is seen immediately that the residue Glu140 that is labeled with NCCD is located deeper into the membrane than is residue Cys54 that is labeled by 5-MSL. From the calibration that is given by the n-SASL labels in Figure 5, it can be concluded that Glu140 is located around the C9−C10 position of the lipid chains in the membrane and that Cys54 is located at around the C5−C6 lipid chain position.

Double Spin-Labeling Experiments. To determine whether the spin-labeled residues on the protein are exposed to the lipid, double-labeling experiments were carried out (cf. refs *12* and *28*). The 16-kDa proteolipid was covalently labeled at a specific residue, with either the 5-MSL or the NCCD spin label. Simultaneously, the lipid environment of the membrane was doped with one of the n-SASL or TS spin probes bearing the spin label at a specific position in the lipid chain. The ESR spectra of 16 kDa-membranes spin-labeled with 5-MSL and 5-SASL, or with NCCD and 11-SASL, are given in Figures 6A and 6B, respectively. The upper of each pair of spectra in Figures 6A and 6B are the conventional in-phase V_1-ESR spectra (solid lines), and the lower of each pair are the second harmonic, 90°-out-of-phase V_2' ST-ESR spectra.

It is seen from Figures 6A and B that the conventional ESR spectra of the double-labeled samples (solid black lines) can be fit with a high degree of precision by a superposition (grey lines) of the individual spectra from the two singly labelled samples. The latter spectra are given by the dotted lines for protein labeling alone and by the dashed lines for lipid labeling alone. Any spin−spin interactions between the protein and lipid labels are too weak to have an appreciable effect on the line widths in the conventional V_1-ESR spectra of the double-labeled samples. Least-squares fitting of the sum of the individual component spectra from the singly labelled samples to the composite spectrum of the doubly labelled sample, together with double integrals of the spectra, therefore, gives the fraction, *f*, of the total spin label spectral intensity that is contributed by the protein spin label. These values are required later for analysis of the effects of spin−spin interactions on the ST-ESR spectral intensities of the doubly labelled samples.

Because the conventional ESR spectra of the double-labeled samples are insensitive to mutual spin−spin interactions, the second-harmonic, out-of-phase saturation-transfer ESR spectra of these samples were recorded. The integrated intensities, I_{ST}, of the ST-ESR spectra are far more sensitive to weak spin−spin interactions than are the conventional ESR line widths because the former are determined by the spin−lattice relaxation time, T_1, rather than by the spin−spin relaxation time, T_2 (see ref *27*). In the lower of each pair of spectra in Figures 6A and 6B, the two-component ST-ESR spectra from the double-labeled samples (black solid lines) are compared with the sum of the ST-ESR spectra from the individual single-labeled samples, i.e., protein and lipid (grey solid lines). For this comparison, the relative intensities of the two spectral components, that were determined from the conventional ESR spectra, i.e., $f/(1 - f)$, were used for

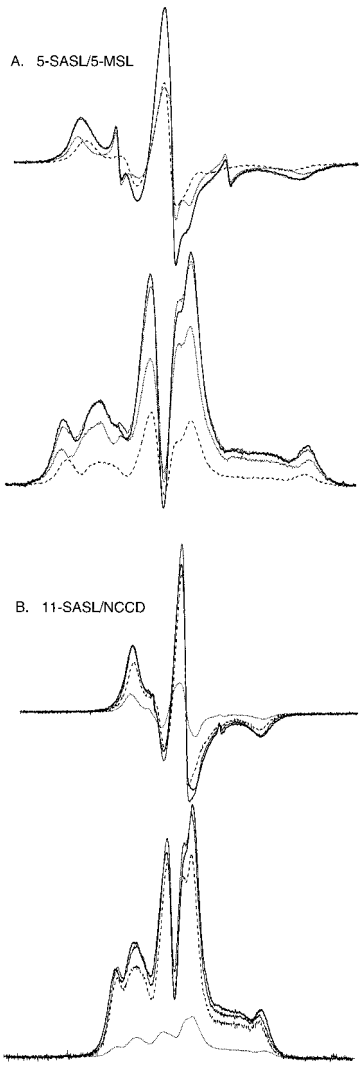

FIGURE 6: Conventional V_1- and saturation-transfer V_2'-ESR spectra (upper and lower of each A and B pair, respectively) of double spin-labeled (protein and lipid) 16-kDa proteolipid membranes from *Nephrops norvegicus*. Solid lines are the spectra from the double-labeled samples; dotted lines are from samples in which only the protein is labeled; and dashed lines are from samples containing only the spin-labeled lipid probe. The gray lines, superimposed on the solid black lines, represent the sum of the spectra from the individual protein- or lipid- singly labelled samples. The summed conventional spectra (upper of each pair) are an optimized fit to the spectrum of the double-labeled sample; individual normalized ST-ESR spectra (lower of each pair) are summed in the same ratio. A. Membranes covalently labeled with the maleimide spin label, 5-MSL, and doped with the 5-SASL stearic acid spin probe. *f*(5-SASL) = 0.5. Total scan width = 100 G. B. Membranes labeled with NCCD and doped with 11-SASL. *f*(11-SASL) = 0.8. Total scan width = 160 G. T = 5 °C.

performing the addition. It is seen that there are more significant differences between the summed and double-labeled ST-ESR spectra than is the case for the conventional ESR spectra (compare upper and lower spectra in Figures 6A and 6B). These differences can be attributed to mutual spin−spin interactions between the spin-labeled lipid and spin-labeled protein in the double-labeled samples.[2]

A more direct measure of the mutual spin−spin interactions is afforded by the difference, ΔI_{ST}, between the value, I_{ST}, of the normalized ST-ESR intensity of the double-labeled sample and the value, predicted from linear additivity of the individual component intensities, $I_{ST,P}{}^{o}$ and $I_{ST,L}{}^{o}$, from the

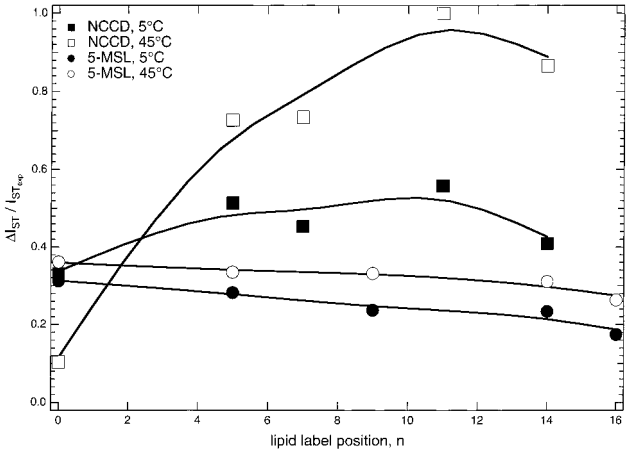

FIGURE 7: Intensity of the ST-ESR spectra from 16-kDa membranes spin-labeled simultaneously with either 5-MSL (circles) or NCCD (squares) and one of the n-SASL stearic acid spin probes (or the TS probe, located at $n = 0$). Data are given for the difference, ΔI_{ST}, of the experimental values of I_{ST} for the double-labeled sample from those predicted from measurements on the singly labelled samples (i.e., for no spin exchange). Filled symbols are for a sample temperature of 5 °C and open symbols for 45 °C. ΔI_{ST}, normalized to the value of I_{ST} for the double-labeled sample, is plotted as a function of the position, *n*, of the spin label on the lipid chain.

single-labeled samples, protein and lipid, respectively:

$$\Delta I_{ST} = f I^{o}_{ST,P} + (1 - f) I^{o}_{ST,L} - I_{ST} \qquad (4)$$

where *f* is the fractional population of the spin-labeled protein species, relative to the total spin-label population, in the double-labeled samples. The latter is determined from the conventional spectra (upper spectrum of each pair in Figure 6), which are insensitive to mutual spin−spin interactions. The values of ΔI_{ST} for the two series of membrane samples with protein labeled either by 5-MSL or by NCCD, and with the different n-SASL lipid probes, are given in Figure 7. The values of the decrease, ΔI_{ST}, in intensity of the ST-ESR spectra of the double-labeled samples, relative to that expected in the absence of mutual spin−spin interactions, are greater than zero for both the 5-MSL and NCCD-labeled samples. This indicates that both the 5-MSL label (on Cys54) and the NCCD label (on Glu140) are accessible for effective spin−spin interaction with spin-labeled stearic acid probes in the membrane lipid phase. The implication of these results is that putative transmembrane helix 2 contacts the lipid chains in the membrane and is oriented such that Cys54 and equivalent residues in the putative helical structure at least partially face outward, toward the lipid, in the hexameric 16-kDa channel complexes. Exactly similar conclusions are reached also with regard to putative transmembrane helix 4 and the orientation of residue Glu140. These latter results are in agreement with mutagenesis, chemical modification and cross linking studies (*28*).

[2] Heisenberg spin exchange between spin labels provides a cross-relaxation mechanism for alleviation of saturation, rather than a true spin−lattice relaxation sink that would be provided by a fast-relaxing paramagnetic species with much shorter T_1. Transfer of saturation occurs from spin labels at the instantaneous position of the spectrum irradiated to spin labels at spectral positions that are not irradiated, by this cross-relaxation process (e.g., refs *12*, *25*, *29*). Explicit expressions for the reduction in effective T_1-relaxation time by this mechanism in continuous wave experiments are given in the Appendix.

The—at first somewhat surprising—result that a glutamic acid residue is located in a hydrophobic, lipid-chain environment is supported by the finding that the binding of a hydrophobic dibutyltin flavone is inhibited by the covalent binding of DCCD (*8*). Also, DCCD itself, which binds specifically to Glu140 of the 16-kDa proteolipid (*3*), is a rather hydrophobic compound. Evidently, the side chain of Glu140 remains protonated (as is required for the reaction with DCCD), whenever it is in contact with lipid. Only when this residue comes in contact with the *υph1p* subunit of the intact V-ATPase, does it become unprotonated, in agreement with the proposed rotary mechanism for catalysis (see ref *28*).

The positional dependence of the spin−spin interactions between the n-SASL spin probes and the 5-MSL or NCCD spin labels that are attached to either Cys54 or Glu140, respectively, of the 16-kDa protein in *Nephrops* membranes is seen from Figure 7. Also included in Figure 7 are corresponding results for Tempo stearate (TS), a lipid spin-labeled in the polar headgroup region. It should be emphasized (see Materials and Methods) that the samples used in a given series with different n-SASL spin probe positional isomers were all derived from the same batch of covalently spin-labeled membranes (with either 5-MSL or NCCD). Care was taken also to ensure that, as near as possible, the different n-SASL spin probes were all incorporated at the same relative concentration. Therefore, both the spin concentration of the individual spin-labeled components and the total spin label concentration were maintained constant. This point is important because the mutual spin−spin interactions in the double-labeled samples are determined both by the relative spin concentrations of the two components and by the total spin label concentration (*12*, *29*).

It should be noted that the absolute values of ΔI_{ST} cannot be compared between the 5-MSL and NCCD series, however, because the degree of protein (and lipid) spin labeling, although constant within a given series, can differ between the two series. For NCCD bound to the 16-kDa protein, it is found that the maximum reduction, ΔI_{ST}, in intensity of the ST-ESR spectrum for the double-labeled samples occurs with n-SASL spin probes for which $n = 10-11$ (see Figure 7). This locates the NCCD spin label on Glu140 deep in the membrane interior, in the region of the C10−C11 position of the lipid chains. This location is reasonably consistent with that obtained from the paramagnetic quenching by aqueous Ni^{2+} ions (see Figure 5). For the experimental series with membranes covalently labeled with 5-MSL, the positional profile of the values of ΔI_{ST} does not peak so clearly as for the NCCD-labeled membranes (see Figure 7). However, the positional trend in the relaxation enhancement suggests that the 5-MSL spin label on Cys54 of the 16-kDa protein is located less deeply in the membrane than is the NCCD spin label on Glu140. The latter finding is consistent with the results obtained from the paramagnetic relaxation enhancement by aqueous Ni^{2+} ions, which places the 5-MSL spin label on Cys54 in the region of the C5−C6 position of the lipid chains (see Figure 5).

Potentially, a more precise definition of the mutual spin−spin interactions in the double-labeled samples can be obtained from the effective spin exchange frequencies, τ_{ex}^{-1}, between the spin-labeled lipid and spin-labeled 16-kDa protein. This assumes that the whole of the spin−spin

Table 1: Saturation Transfer ESR Integral ($I_{ST} \times 10^2$) of 16-kDa Membranes Doubly and Singly Spin-Labeled with the Maleimide Spin Label (MSL) and Stearic Acid Spin Labels (n-SASL)[a]

	I_{ST} ($\times 10^2$)			f(MSL)	I_{ST}^o (x10^2)	$T_{1,P}^o\tau_{ex}^{-1}$
n	MSL	n-SASL	MSL+n-SASL		(MSL+n-SASL)$_o$	
5 °C						
5	0.647	0.457	0.466	0.50	0.55	0.50
9	0.647	0.531	0.517	0.50	0.59	0.35
14	0.647	0.388	0.434	0.52	0.52	0.59
16	0.647	0.388	0.513	0.62	0.55	0.19
45 °C						
5	0.254	0.148	0.171	0.50	0.20	0.48
9	0.254	0.141	0.172	0.50	0.20	0.40
14	0.254	0.111	0.151	0.52	0.19	0.68
16	0.254	0.162	0.192	0.62	0.22	0.43

[a] f(MSL) is the fractional population of the MSL label in the doubly labelled (MSL+n-SASL) samples. (MSL+n-SASL)$_o$ is the value of $I_{ST} \times 10^2$ predicted for the doubly labeled sample in the absence of spin exchange, using the values from the singly labeled samples. $T_{1,P}^o\tau_{ex}^{-1}$ is the normalized exchange frequency (see eq A5).

interaction can be attributed to a collision-controlled Heisenberg exchange mechanism (cf. ref *12*). The exchange (or collision) frequencies may then be calculated from the measured values of ΔI_{ST}, as is described in the Appendix. The resulting values for the exchange frequencies, τ_{ex}^{-1}, normalized to the spin−lattice relaxation time, $T_{1,P}^o$, of the spin-labeled protein are given in Table 1 for the 5-MSL spin label series with different lipid spin probes. With the exception of the data for 14-SASL, these data are consistent with the 5-MSL label being located in the region of C5 of the lipid chain. The effective exchange frequencies increase with increasing temperature, for lipids labeled close to the terminal methyl of the chain (see Table 1). However, they change relatively little for those lipids closer to the carboxyl polar head, presumably because this region of the chain is restricted in its motion by the close-packed protein arrays. The overall larger values of ΔI_{ST} for the NCCD series than for the 5-MSL series (see Figure 7) suggest that the degree of labeling is higher than in the case of the 5-MSL series. The result of this higher level of labeling for the NCCD series is that the effective exchange frequencies all lie beyond the range of applicability of the analysis for slow exchange that is given in the Appendix.

CONCLUSIONS

Nonlinear ESR spectroscopy combined with site-directed spin-labeling at specific reactive sites in native membranes from *Nephrops norvegicus* has succeeded in delineating various crucial aspects of the intramembranous assembly of the 16-kDa proteolipid proton channel. This method provides an extension of the conventional systematic approach to site-directed spin-labeling (see ref *30*) that is possible when unique sites are differentially sensitive to complementary spin label reagents, e.g. maleimide and NCCD. A wide spectrum of different spin−spin interactions that are readily detectable by nonlinear ESR methods has been shown to be capable of providing vital information on the intramembranous structure and assembly of the 16-kDa proteolipid. The dependence of the spin label saturation properties on level of labeling is found to be sensitively dependent on the oligomeric state of assembly of the channel protein in the membrane and to be quantitatively consistent with a hexameric assembly of the protein monomers. Both paramagnetic relaxation enhancement and protein−lipid interactions in double-spin labeled membranes indicate that the Glu140 residue on putative transmembrane helix-4 is located deeper in the membrane than is Cys54 on putative transmembrane helix-2. The Glu140 residue that is essential to proton transport is found to be accessible from the lipid phase of the membrane, as is required by the rotary mechanism proposed for the coupled V-ATPase activity.

ACKNOWLEDGMENT

We thank Frau Brigitta Angerstein and Ms. Pauline Mclean for their excellent technical support in synthesizing the NCCD spin label and preparation of membrane material, respectively.

APPENDIX 1. ANALYSIS OF TWO-COMPONENT ST-ESR SPECTRAL INTENSITIES

For an ST-ESR spectrum composed of two components, the normalized integrated intensity, I_{ST}, is given by linear additivity of the intensities from the two components P and L (*24*):

$$I_{ST} = f I_{ST,P} + (1 - f) I_{ST,L} \tag{A1}$$

where f is the fractional population of component P and $I_{ST,i}$ is the normalized value of the saturation transfer integral for component i (with $i \equiv P$ or L). The normalized integral intensity, $I_{ST,i}$, contributed by each component i in the ST-ESR spectrum is approximately proportional to the effective spin−lattice relaxation time, $T_{1,i}^{eff}$, of the spin labels giving rise to that component (*9*, *23*):

$$I_{ST,i} = (I_{ST,i}^o / T_{1,i}^o) T_{1,i}^{eff} \tag{A2}$$

where $I_{ST,i}^o$ and $T_{1,i}^o$ are the ST-ESR integral and effective T_1, respectively, in the absence of spin exchange between the two components. The effective spin−lattice relaxation rate, $1/T_{1,P}^{eff}$, of spin label P in the presence of Heisenberg exchange with the spin label L, and the corresponding relaxation rate, $1/T_{1,L}^{eff}$, for spin label L are respectively given by (*12*):

$$\frac{T_{1,P}^o}{T_{1,P}^{eff}} = 1 + \frac{(1 - f) T_{1,P}^o \tau_{ex}^{-1}}{1 + f T_{1,L}^o \tau_{ex}^{-1}} \tag{A3}$$

$$\frac{T_{1,L}^o}{T_{1,L}^{eff}} = 1 + \frac{f T_{1,L}^o \tau_{ex}^{-1}}{1 + (1 - f) T_{1,P}^o \tau_{ex}^{-1}} \tag{A4}$$

where τ_{ex}^{-1} is the Heisenberg spin exchange frequency which is linearly related, by the bimolecular rate constant for spin exchange, to the total spin label concentration (*29*). Substituting in eq A1 from eqs A3 and A4, together with eq A2, then yields the following expression for the Heisenberg exchange frequency:

$$\tau_{ex}^{-1} = \frac{\Delta I_{ST}}{f(1 - f)(T_{1,L}^o I_{ST,L}^o + T_{1,P}^o I_{ST,P}^o) - [f T_{1,L}^o + (1 - f) T_{1,P}^o] \Delta I_{ST}} \tag{A5}$$

where $\Delta I_{ST} = f I_{ST,P}^o + (1 - f) I_{ST,L}^o - I_{ST}$ is the reduction

in the value of I_{ST} for the double-labeled sample over that predicted in the absence of Heisenberg spin exchange interaction between the two spin labels. The relation $T_{1,L}{}^{o} = (I_{ST,L}{}^{o}/I_{ST,P}{}^{o})T_{1,P}{}^{o}$ from eq A2 can be used to express the exchange frequency in terms of the single scaled value, $T_{1,P}{}^{o}\tau_{ex}{}^{-1}$, that then can be obtained from the measured ST-ESR intensities and the value of *f*.

REFERENCES

1. Holzenburg, A., Jones, P. C., Franklin, T., Páli, T., Heimburg, T., Marsh, D., Findlay, J. B. C., and Finbow, M. E. (1993) *Eur. J. Biochem. 213*, 21−30.
2. Harrison, M. A., Jones, P. C., Kim, Y.-I., Finbow, M. E., and Findlay, J. B. C. (1994) *Eur. J. Biochem. 221*, 111−120.
3. Finbow, M. E., Eliopoulos, E. E., Jackson, P. J., Keen, J. N., Meagher, L., Thompson, P., Jones, P. C., and Findlay, J. B. C. (1992) *Protein Eng. 5*, 7−15.
4. Hirata, R., Graham, L. A., Takatsuki, A., Stevens, T. H., and Anraku, Y. (1997) *J. Biol. Chem. 272*, 4795−4803.
5. John, S. A., Saner, D., Pitts, J. D., Holzenburg, A., Finbow, M. E., and Lal, R. (1997) *J. Struct. Biol. 120*, 22−31.
6. Páli, T., Finbow, M. E., Holzenburg, A., Findlay, J. B. C., and Marsh, D. (1995) *Biochemistry 34*, 9211−9218.
7. Jones, P. C., Harrison, M. A., Kim, Y.-I., Finbow, M. E., and Findlay, J. B. C. (1995) *Biochem. J. 312*, 739−747.
8. Hughes, G., Harrison, M. A., Kim, Y.-I., Griffiths, D. E., Finbow, M. E., and Findlay, J. B. C. (1996) *Biochem. J. 317*, 425−431.
9. Páli, T., Livshits, V. A., and Marsh, D. (1996) *J. Magn. Reson. B113*, 151−159.
10. Livshits, V. A., Dzykovski, B. G., and Marsh, D. (1999) Mechanism of relaxation enhancement of spin labels in membranes by paramagnetic ion salts. Dependence on 3*d* and 4*f* ions and on the anions. Submitted for publication.
11. Páli, T., Bartucci, R., Horváth, L. I., and Marsh, D. (1992) *Biophys. J. 61*, 1595−1602.
12. Snel, M. M. E., and Marsh, D. (1994) *Biophys. J. 67*, 737−745.
13. Finbow, M. E., Buultjens, T. E. J., Lane, N. J., and Pitts, J. D. (1984) *EMBO. J. 3*, 2271−2278.
14. Leitch, B., and Finbow, M. E. (1990) *Exp. Cell Res. 190*, 218−226.
15. Azzi, A., Bragadin, M. A., Tamburro, A. M., and Santato, M. (1973) *J. Biol. Chem. 248*, 5520−5526.
16. Girvin, M. E., and Fillingame, R. H. (1994) *Biochemistry 33*, 665−674.
17. Hemminga, M. A., De Jaeger, P. A., and Marsh, D. (1984) *J. Magn. Reson. 59*, 160−163.
18. Eibl, H., and Lands, W. E. M. (1969) *Anal. Biochem. 30*, 51−57.
19. Lowry, O. H., Rosebrough, N. J., Farr, L., and Randall, R. J. (1951) *J. Biol. Chem. 193*, 265−275.
20. Fajer, P., and Marsh, D. (1982) *J. Magn. Reson. 49*, 212−224.
21. Sachse, J.-H., King, M. D., and Marsh, D. (1987) *J. Magn. Reson. 71*, 385−404.
22. Freed, J. H. (1976) in *Spin Labeling. Theory and Applications* (Berliner, L. J., Ed.) pp 53−132, Academic Press Inc., New York.
23. Marsh, D., and Horváth, L. I. (1992) *J. Magn. Reson. 97*, 13−26.
24. Horváth, L. I., and Marsh, D. (1983) *J. Magn. Reson. 54*, 363−373.
25. Marsh, D. (1992) *Appl. Magn. Reson. 3*, 53−65.
26. Langen, R., Isas, J. M., Luecke, H., Haigler, H. T., and Hubbell, W. L. (1989) *J. Biol. Chem. 273*, 22453−22457.
27. Marsh, D., Páli, T., and Horváth, L. I. (1998) in *Biological Magnetic Resonance*, Vol. 14. *Spin-Labeling: The Next Millenium* (Berliner, L. J., Ed.) Ch. 2, pp 23−82, Plenum Press, New York.
28. Harrison, M. A., Powell, B., Páli, T., Marsh, D., Finbow, M. E., and Findlay, J. B. C. (1999) The subunit c glutamic acid residue responsible for proton translocation in the vacuolar H^{+}-ATPase has contact with the hydrophobic core of the membrane bilayer. Submitted for publication.
29. Marsh, D. (1992) *J. Magn. Reson. 99*, 332−337.
30. Hubbell, W. L., and Altenbach, C. (1994) in *Membrane Protein Structure: Experimental Approaches* (White, S. H., Ed.) pp 224−248, Oxford University Press, New York.

BI991459C